Trans. of the Korean Hydrogen and New Energy Society(2015. 4), Vol. 26, No. 2, pp. 148~155
DOI: http://dx.doi.org/10.7316/KHNES.2015.26.2.148
ISSN 1738-7264
eISSN 2288-7407

다양한 온도에서 합성한 전기방사 $LaCoO_3$ 페롭스카이트 나노섬유의 알칼리용액에서 산소환원 및 발생반응에 대한 전기화학 특성

로페즈 카린[1] · 선호정[2] · 박경세[3] · 엄승욱[4] · 심중표[1†]
[1]군산대학교 나노화학공학과, [2]군산대학교 신소재공학과, [3]군산대학교 화학과, [4]한국전기연구원 전지연구센터

Electrochemical Characterization of Electrospun $LaCoO_3$ Perovskite Nanofibers Prepared at Different Temperature for Oxygen Reduction and Evolution in Alkaline Solution

KAREEN J. LOPEZ[1], HO-JUNG SUN[2], GYUNGSE PARK[3], SEUNGWOOK EOM[4], JOONGPYO SHIM[1†]
Dpartment of [1]Nano & Chemical Engineering, [2]Material Science & Engineering and [3]Chemistry, Kunsan National University, Jeonbuk, 573-701, Korea
[4]Battery Research Center Korea Electrotechnology Research Institute, Changewon, Gyeongnam, 641-120, Korea

Abstract >> Electrospun $LaCoO_3$ perovskite nanofibers were produced for the air electrode in Zn-air rechargeable batteries using electrospinning technique with sequential calcination. The final calcination temperature was varied from 500 to 800 °C in order to determine its effect on the physical and electrochemical properties of the prepared $LaCoO_3$ perovskite nanofibers. The surface area of the electrospun $LaCoO_3$ perovskite nanofibers were observed to decrease with increasing final calcination temperature. Electrospun $LaCoO_3$ perovskite nanofibers calcined with final calcination temperature of 700 °C had the best electrocatalytic activity among the prepared perovskite nanofibers.

Key words : Zn-air battery(아연공기전지), air electrode(공기극), perovskite(페롭스카이트), $LaCoO_3$, nanofiber(나노섬유), oxygen reduction(산소환원), oxygen evolution(산소발생)

1. Introduction

The rising demand for portable electrical gadgets and machines increases the need for higher energy storage and conversion devices. In order to meet this demand, several studies are made to develop the current existing batteries and to be able to deal with their limitations and disadvantages. Among these batteries, zinc-air battery, a type of metal-air battery, has attracted huge interest owing to its desirable properties such as its high energy density, economical and safe production, and environmentally-benign materials and operation[1-8].

The commercialized zinc-air primary batteries have

†Corresponding author : jpshim@kunsan.ac.kr
Received : 2015.04.14 in revised form : 2015.04.24 Accepted : 2015.04.30

been employed in several years for applications that need long-term battery life, because of the difficulty and costly frequent replacements like in the railroad crossing signals, and light weight devices, examples are hearing aids and medical equipments. The rechargeable type zinc-air battery, or ZARB or secondary zinc-air battery, is still on its development stage due to the many drawbacks that hinder its commercial use. One of the major downside in zinc-air battery is its low performance caused by slow reaction kinetics related with the oxygen reduction reaction (ORR) and oxygen evolution reaction (OER) of the cathode electrode. The rate of ORR and OER in the cathode is influenced by the kind of catalyst used. At present, platinum and its alloys are utilized as catalysts for ORR while Pt and Ir, Ru, Ni oxides/ hydroxides for OER. These catalysts, however, aside from expensive due to limited resources, still lack the catalytic activity to improve the ORR/OER in the cathode. For zinc-air rechargeable battery and other metal-air batteries, in general, a good catalyst is considered by effectively catalyzing both ORR and OER in the cathode while the electrical charge and discharge takes place; such catalysts are called bifunctional catalyst[6-13].

Catalysts of perovskite-type metal oxides have shown bifunctional catalytic activity which makes it an attractive substitute for noble metals and their alloys in catalyzing ORR and OER. $LaMO_3$ perovskites (M = transition metal) have been widely studied because of their low cost and high catalytic activity comparable to noble metals. Additional advantages of utilizing perovskites are the simplicity of preparation and its flexibility enabling it to achieve the specific properties desired for different applications, examples of these properties are conductivity and surface area. Among the $LaMO_3$ perovskites, one of the most studied is $LaCoO_3$ (LCO) because it is one of the perovskite that have the highest catalytic activity and the best rechargeability compared to other $LaMO_3$ perovskites with notable stability. Several researches are made to optimize the catalytic activity of LCO by using different techniques of preparation and by varying the calcination temperature. A recent technique utilized in perovskite preparation is electrospinning, a method that utilizes high voltage to produce fibers on a nanoscale range from a polymeric solution. Perovskite preparation using electrospinning technique usually uses a polymer that acts as a template and as the chelating material for the metal salts[14-19].

In the current study, the influence of the calcination temperature to the physical properties and the catalytic activity of the LCO perovskite nanofibers for ORR/ OER in zinc-air battery was determined. LCO perovskite precursor nanofiber is prepared through electrospinning using poly (vinyl pyrrolidone) (PVP) as the polymeric template[19].

2. Experimental

The synthetic procedure of LCO perovskite nanofibers is composed of two parts; preparation of LCO perovskite nanofiber precursor, and heat treatment. The first part consists of the preparation of the polymeric solution containing lanthanum and cobalt, and the electrospinning of the polymeric solution. The solution was prepared by dissolving the metal salts in deionized water, in this case, the reagents used are lanthanum nitrate hexahydrate ($La(NO_3)_3 \cdot 6H_2O$) and cobalt nitrate hexahydrate ($Co(NO_3)_2 \cdot$

$6H_2O$). The solution was stirred for 12 hrs at room temperature, and then, PVP (MW = 1,300,000) was added. It was stirred until PVP was completely dissolved resulting to a viscous clear pink polymeric solution[18,19]. The amount of PVP added is twice the theoretical amount of $LaCoO_3$ perovskite while the deionized water is five times the amount of PVP.

The prepared solution was transferred into a plastic syringe which was then placed onto the syringe pump connected to the nozzle of the electrospinning set-up. Electrospinning is done with a voltage of 15 kV, flow rate of 1.1 mL/h and tip-to-collector distance of 15 cm. The resulting fibrous mat was dried at 60 ^oC in an oven before heat treatment[18,19].

The heat treatment of the dried fibrous mat comprises of three stages; the first stage is heating from 60 ^oC and increasing the temperature by 25 ^oC every 10 mins until temperature reached 200 ^oC, the second stage is heating at 200 ^oC for 2 hrs then increasing the temperature by 25 ^oC every 10 mins until it reaches 400 ^oC, and lastly, heat treatment at 400 ^oC for 2 hrs and then increasing the temperature by 25 ^oC every 10mins until the final temperature is reached in which it remained constant for another 2 hrs. In order to determine the effect of the final calcination temperature to the physical and chemical properties of electrospun LCO, the final temperature was varied to 500, 600, 700 and 800 ^oC, respectively.

The characterization includes weight loss with respect to temperature increase by thermal gravimetric analysis (TGA, SDT Q-600), morphology by field-emission scanning electron microscopy (FE-SEM, Hitachi S-4800), crystalline structure using X-ray diffraction (XRD, PANalytical), surface area by means of Brunauer, Emmett and Teller (BET) analysis, and particle size distribution through particle size analysis (PSA, HELOS/RODOX & SUCELL with Sympatec GmbH).

The catalytic activity of electrospun LCO for ORR/OER is determined by cyclic voltammetry which was conducted via potentiostat/ galvanostat (WBCS 3000, WonATech) for 5 cycles with voltage range of 0.8 to 2.5 V and a scan rate of 1 mV/s in a three electrode system that composed of Zn wire and Pt mesh as the reference and counter electrodes while the working electrode is a prepared cathode containing the electrospun LCO perovskite as the catalyst[15,20,21]. The working electrode is prepared by spraying, on a wet-proof carbon paper (Ballard Avcarb P50), the homogenized catalyst in a 3:1 mixture of deionized water and ethanol containing a drop of triton X-100 as the surfactant and PTFE as the binder. Then, it was dried at 60^oC and the surfactant was removed by washing with distilled water followed by acetone and subjected to drying again. Once dried, it was submitted to hot-press at 60 ^oC and 5 MPa and then it was subjected to heat at 330 ^oC for 30 mins. The electrode was weighed and cut into circle with a diameter of 2 cm. Then, it was placed in a cell frame to which 8 M KOH solutions was added as the electrolyte.

3. Results and Discussion

The result of the thermal gravimetric analysis (TGA) shown in Fig. 1 is used as the basis in choosing the minimum final temperature for calcination. The figure shows that before reaching 500 ^oC mark, the weight loss percent has been consistent. With regards to this observation, it has the possibility that after the removal of unwanted carbon constituents before reaching that

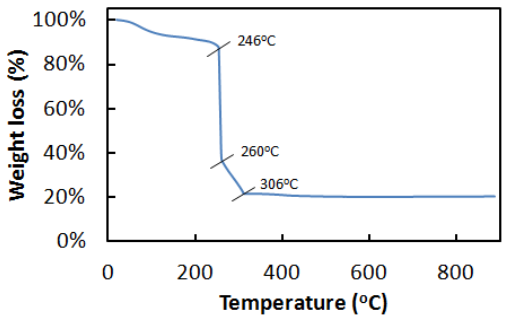

Fig. 1 TGA of PVP-$LaCoO_3$ precursor nanofibers in air atmosphere

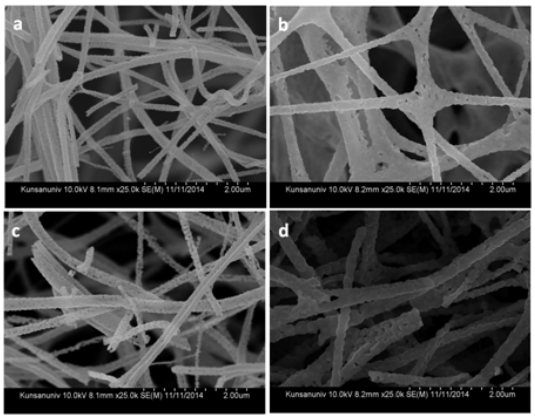

Fig. 2 SEM images of electrospun $LaCoO_3$ nanofibers calcined at different temperature. a) 500 °C, b) 600 °C, c) 700 °C, and d) 800°C

temperature, the formation of perovskite-type crystal structure may have started. The graph of percent weight loss shown in Fig. 1 can be divided into two major parts, the loss of free and coordinated water molecules below 250 °C, and the decomposition of PVP and metal nitrates between 250 °C and 480 °C[22-24].

The PVP-LCO precursor nanofibers sequentially calcined at final temperatures of 500, 600, 700 and 800 °C, respectively, are represented as LCO-500, LCO-600, LCO-700, and LCO-800. The morphology of the calcined samples is shown in Fig. 2 in which it can be observed that the fibers are composed of smaller particles that agglomerated. LCO-500 and

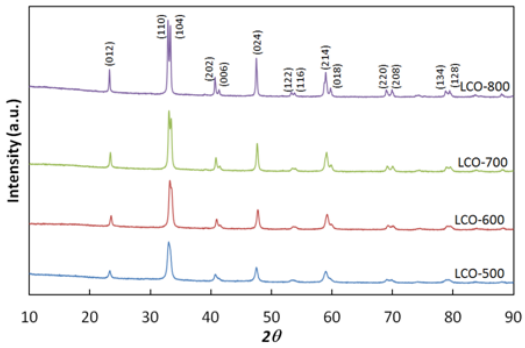

Fig. 3 XRD patterns of electrospun $LaCoO_3$ nanofibers calcined at different temperature

LCO-600 (Fig. 2a-b) have almost same fiber diameters, although, the range of fiber diameter of LCO-500 is slightly lower than that of LCO-600 which is manifested by the presence of some significantly smaller fibers in Fig. 2a. The fiber diameters of LCO-700 in Fig. 2c are considerably bigger than LCO-500 and LCO-600 while LCO-800 (Fig. 2d) having fiber diameters of less than 500 nm is observed to have the largest fibers among the four samples.

Fig. 3 shows the result of the XRD analysis of the electrospun PVP-LCO precursor nanofibers for different calcination temperature. The XRD peaks correspond to perovskite-type crystals[25,26] with respect to the reference pattern obtained using the HighScore Plus software with Rietveld refinement. In addition, it was determined that the samples obtained are of single-phase perovskite materials having rhombohedral crystal system (ICOD 01-084-0848) with R-3c space group. The porosity of the calcined LCO perovskites decreases with increasing final calcination temperature as supported by the measured BET surface area shown in Table 1 in which LCO-500 has the highest BET surface area of 11.41 m^2/g followed by LCO-600 and LCO-700 with 9.14 and 8.50 m^2/g and lastly, LCO-800 with 5.94 m^2/g. This leads to the possibility that the

Table 1 Surface area, current density, mass activity and specific activity of $LaCoO_3$ perovskite nanofibers calcined at different temperature for ORR and OER

	Surface area (m^2/g)	ORR			OER		
		I (mA/cm^2)	I_{MA} (mA/mg)	I_{SA} ($\mu A/cm^2$)	I (mA/cm^2)	I_{MA} (mA/mg)	I_{SA} ($\mu A/cm^2$)
LCO-500	11.4	5.9	6.2	54.4	32.2	33.9	297.2
LCO-600	9.1	26.5	34.5	378.2	97.1	126.8	1387.9
LCO-700	8.5	21.4	45.1	531.0	83.2	175.7	2067.5
LCO-800	5.9	16.2	32.0	538.3	62.3	123.4	2078.5

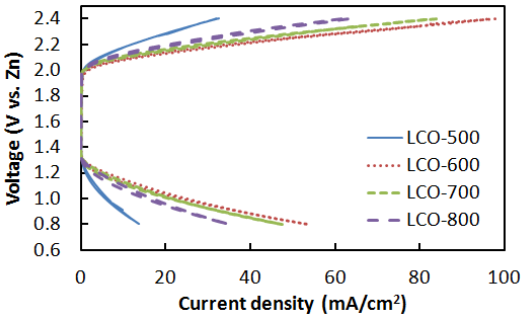

Fig. 4 ORR and OER performance of electrospun $LaCoO_3$ nanofibers calcined at different temperature. 8M KOH solution

porosity of the calcined LCO perovskites enabled the particles to get stuck together forming a bigger particle.

Fig. 4 shows the electrocatalytic performance of the electrospun LCO perovskite nanofibers calcined with different temperatures and loaded as a catalyst on prepared electrodes. In the figure, LCO-600 obtained the highest current density followed by LCO-700 and LCO-800, while LCO-500 has the lowest current density. The comparison of their respective ORR and OER performance against Zn, with an electrode having an area of 1 cm^2, the amount of the catalyst loaded, in mg/cm^2, and BET surface area of catalysts is shown in Table 1 where in I corresponds to the current density, I_{MA} is for the mass activity, and I_{SA} is for the specific activity of the respective catalyst[15]. The current density, I, obtained at 1.0 V (vs. Zn) is used to evaluate the ORR performance of the catalysts in which LCO-600 appears to have best catalytic performance. However, the electrocatalytic activity for ORR of LCO-600 is only second to LCO-700 with respect to mass activity, which is the current density per the amount of the catalyst loading. Moreover, LCO-800 has a lower performance than LCO-600 and LCO-700 in terms of mass activity, while it has the highest specific activity among the four electrocatalysts wherein specific activity is the current density (mA/cm^2) available to catalyze. LCO-500 is observed to have the least electrocatalytic performance for both ORR and OER as it has the lowest current density in spite of its high surface area caused by its smaller particles and porous morphology. On the other hand, the performance for the OER is evaluated at 2.4 V (vs. Zn) wherein LCO-700 has a higher specific activity than LCO-600.

Fig. 5 shows the plot of the mass activity against the final calcination temperature for both the ORR and OER, wherein the mass activity increased with increasing temperature. However, the mass activity decreased when the final calcination temperature is increased to 800 ^oC. Likewise, the specific activity increased with increasing temperature as shown in Fig. 6, although the increase in the specific activity at 800 ^oC is gradual. On the contrary, it was observed that the specific activity decreased with increasing surface area

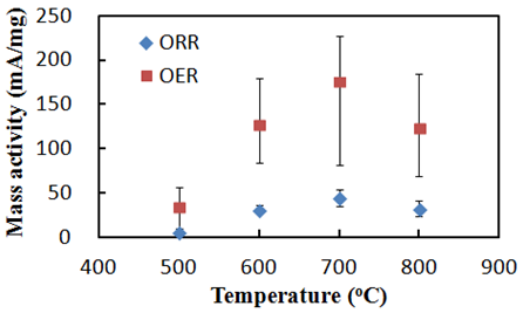

Fig. 5 Mass activity of electrospun $LaCoO_3$ nanofibers as a function of calcination temperature

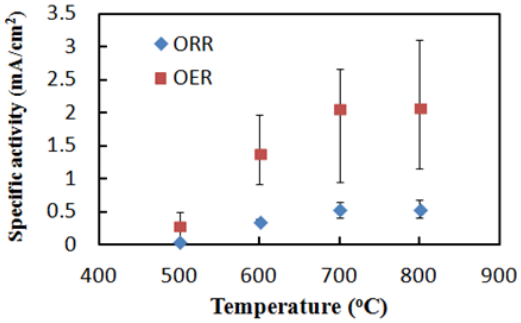

Fig. 6 Specific activity of electrospun $LaCoO_3$ nanofibers as a function of calcination temperature

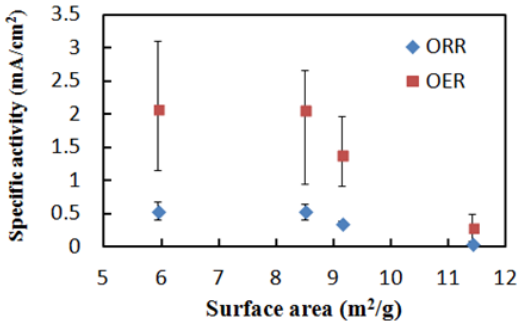

Fig. 7 Specific activity of electrospun $LaCoO_3$ nanofibers as a function of surface area of catalyst

for both ORR and OER as shown in Fig. 7. It means that the catalysts with low surface area calcined at higher temperature are well crystallized and have superior electrocatalytic activity on the surface.

4. Conclusions

Electrospinning was used as an effective method of preparing LCO perovskite fibers having diameters of less than 1.0 μm and it was observed that the use of polymer templates such as PVP is important to attain a nanofiber perovskite. In addition, the sequential calcination is a major step in retaining the nanofiber morphology of the perovskites that were produced by electrospinning because heat treatment after electrospinning tends to break the formed nanofibers into smaller random particles. In terms of calcination temperature, this study shows that the final calcination temperature has a great influence on some important physical properties of the electrospun LCO perovskite, such as the surface area which can greatly affect the electrocatalytic activity of the perovskites by providing enough surfaces for the ORR and OER. Also, the temperature of calcination influence both the ORR and OER performance of the catalysts as it shows that ORR and OER follows the same trend for both the mass and specific activity. Lastly, the electrospun LCO perovskite calcined at 700 °C (LCO-700) shows to have the best electrocatalytic activity as observed from its ORR and OER performance based on the parameters used.

Acknowledgment

This work was supported by the National Research Foundation of Korea Grant funded by the Korean Government (MEST) (NRF-2012-M1A2A2-029538).

References

1. S.-M. Lee, Y.-J.Kim, S.-W. Eom, N.-S. Choi,

K.-W. Kim, S.-B. Cho, “Improvement in self-discharge of Zn anode by applying surface medication for Zn-air batteries with high energy density”, J. Power Sources, Vol. 227, 2013. p. 177.

2. X. Wang, P.J. Sebastian, M.A. Smit, H. Yang, S.A. Gamboa, “Studies on the oxygen reduction catalyst for zinc-air battery electrode”, J. Power Sources, Vol. 124, 2003, p.278.
3. J-S. Lee, S.T. Kim, R. Cao, N-S. Choi, M. Liu, K.T. Lee, J. Cho, “Metal-Air Batteries with High Energy Density: Li-Air versus Zn-Air”, Adv. Energy Materials, Vol. 1, No. 1, 2011, p. 34.
4. J.J. Martin, V. Neburchilov, H. Wang, W. Qu, “Air Cathodes for Metal-Air Batteries and Fuel Cells” IEEE Electrical Power & Energy Conference, 2009.
5. T. Cutler, “A Design Guide for Rechargeable Zinc-air Battery Technology”, Southcon 96 conference, 1996, p. 616.
6. D.U. Lee, J. Scott, H.W. Park, S. Abureden, J.-Y. Choi, Z. Chen, “Morphologically controlled Co_3O_4 nanodisks as practical bi-functional catalyst for rechargeable zinc-air battery applications”, Electrochem. Comm., Vol. 43, No. 6, 2014, p. 109.
7. T-H. Yang, S. Venkatesan, C-H. Lien, J-L. Chang, J-M. Zen, “Nafion/lead oxide- mangaese oxide combined catalyst for use as a highly efficient alkaline air electrode in zinc-air battery”, Electrochim. Acta, Vol. 56, No. 17, 2011, p. 6205.
8. Z. Chen, A. Yu, D. Higgins, H. Li, H. Wang, Z. Chen, “Highly Active and Durable Core-Corona Structured Bifunctional Catalyst for Rechargeable Metal-Air Battery Application”, Nano Lett., Vol. 12, No. 4, 2012, p. 1946
9. M. Li, L. Zhang, Q. Xu, J. Niu, Z. Xia, “N-doped graphene as catalysts for oxygen reduction and oxygen evolution reactions: Theoretical considerations”, J. Catalysis, Vol. 314, 2014, p. 66.
10. M. Prabu, S. Shanmugam, “$NiCo_2O_4$- Graphene Oxide Hybrid as a bifunctional Electrocatalyst for Air Breathing Cathode Material in Metal Air Batteries”, Int. Conf. Adv. Nanomaterials & Emerging Eng. Tech., 2013, p. 468.
11. M. Hilder, B. Winther-Jensen, N.B. Clark, “The effect of binder and electrolyte on the performance of thin zinc-air battery”, Electrochim. Acta, Vol. 69, 2012, p. 308.
12. T. Wang, M. Kaempgen, P. Nopphawan, G. Wee, S. Mhaisalkar, M. Srinivasan, “Silver nanoparticle-decorated carbon nanotubes as bifunctional gas-diffusion electrodes for zinc-air batteries”, J. Power Sources, Vol. 195, No. 13, 2010, p. 4350.
13. Z. Chen, A. Yu, R. Ahmed, H. Wang, H. Li, Z. Chen, “Manganese dioxide nanotube and nitrogen-doped carbon nanotube based composite bifunctional catalyst for rechargeable zinc-air battery”, Electrochim. Acta, Vol. 69, 2012, p. 295.
14. C. Zhu, A. Nobuta, I. Nakatsugawa, T. Akiyama, “Solution combustion synthesis of $LaMO_3$ (M = Fe, Co, Mn) perovskite nanoparticles and the measurement of their electrocatalytic properties for air cathode”, Int. J. Hydrogen Energy, Vol. 38, No. 30, 2013, p. 13238.
15. H-J. Sun, M-Y. Cho, J-C. An, S. Eom, G. Park, J. Shim, “Characterization of $LaCoO_3$ Perovskite Catalyst for Oxygen Reduction Reaction in Zn-air Rechargeable Batteries”, Trans. Kor. Hydrogen New Energy Soc., Vol. 25, No. 4, 2014, p. 436.
16. J. Yuh, L. Perez, W.M. Sigmund, J.C. Nino, “Electrospinning of complex oxide nanofibers”, Physica E, Vol. 37, No. 1-2, 2007, p. 254.
17. X. Dong, J. Wang, Q. Cui, G. Liu, W. Yu, “Fabrication of $LaNiO_3$ Porous Hollow Nanofibers via an Electrospinning Technique”, Modern Applied Science, Vol. 3, No. 1, 2009, p. 75.
18. K. Rida, M.A. Pea, E. Sastre, A. Martinex-Aris,

"Effect of calcination temperature on structural properties and catalytic activity in oxidation reactions of LaNiO3 perovskite prepared by Pechini method", J. Rare Earths, Vol. 30, No. 3, 2012, p. 211.

19. J. Wang, X. Dong, Z. Qu, G. Liu, W. Yu, "Fabrication and Characterization of $LaCoO_3$ nanofibers via an Electrospinning Techniques", Int. J. Chem., Vol. 2, No. 1, 2010, p. 161.
20. S. Ahn, K. Kim, H. Kim, S. Nam, S. Eom, "Synthesis and electrochemical performance of $La_{0.7}Sr_{0.3}Co_{1-x}Fe_xO_3$ catalysts for zinc air secondary batteries", Phys. Scr., Vol. T139, 2010, p. 014014
21. F.W.T. Goh, Z. Liu, T.S.A. Hor, J. Zhang, X. Ge, Y. Zong, A. Yu, W. Khoo, "A Near-Neutral Chloride Electrolyte for Electrically Rechargeable Zinc-Air Batteries", J. Electrochem. Soc., Vol. 161, No. 14, 2014, p. A2080.
22. B. Dong, Z. Li, Z. Li, X. Xu, M. Song, W. Zheng, C. Wang, S.S. Al-Deyab, M. El-Neweby, "Highly Efficient $LaCoO_3$ Nanofibers Catalysts for Photocatalytic Degradation of Rhodamine B", J. Am. Ceram. Soc., Vol. 93, No. 11, 2010, p. 3587.
23. J. Zhao, Y. Cheng, X. Yan, D. Sun, F. Zhu, Q. Xue, "Magnetic and electrochemical properties of $CuFe_2O_4$ hollow fibers fabricated by simple electrospinning and direct annealing", Cryst. Eng. Comm., Vol. 14, No. 18, 2012, p. 5879.
24. B. Sahoo, P.K. Panda, "Preparation and characterization of barium titanate nanofibers by electrospinning", Ceramics International, Vol. 38, No. 6, 2012, p. 5189.
25. M.J. Lee, J.H. Jun, J.S. Jung, Y.R. Kim, S.H. Lee, "Catalytic activities of perovskite-type $LaBO_3$ (B = Fe, Co, Ni) oxides for partial oxidation of methane". Bull. Korean Chem. Soc., Vol. 26, No. 10, 2005, p. 1591.
26. D.K. Kang, Y.I. Lee, J.M. Sohn, "Study on the Selective CO Oxidation Using $La_xCe_{1-x}Co_yCu_{1-y}O_{3-\alpha}$ Perovskite Catalysts", Trans. Kor. Hydrogen New Energy Soc., Vol. 18, No. 1, 2007, p. 32.